Recovery of local density of states using scanning tunneling spectroscopy

M. Passoni, F. Donati, A. Li Bassi, C. S. Casari, and C. E. Bottani
Dipartimento di Chimica, Materiali e Ingegneria Chimica "G. Natta", Center for NanoEngineered Materials and Surfaces (NEMAS) and CNISM-Politecnico di Milano, Via Ponzio 34/3, I-20133 Milan, Italy

(Received 6 October 2008; revised manuscript received 4 December 2008; published 9 January 2009)

Scanning tunneling spectroscopy (STS) provides a unique method for the investigation of the local surface-projected electron density of states (DOS), mostly for its capability of reaching atomic resolution. Such information is contained in a nonobvious way in STS data, and a proper understanding of the overall features of the system (sample+tip) is mandatory in order to obtain quantitative information. Several approaches have been proposed in the literature to tackle this problem. A common feature of these methods is that they are mostly based on a one-dimensional (1D) WKB description of the tunneling current. We present a critical analysis and an extension of the methods so far proposed, with the main goal of applying the results to STS experimental data. This study has been conducted by modeling the tip-sample system within the frame of 1D-WKB theory, investigating key open issues, such as the estimation of required but usually experimentally unknown parameters such as the tip-sample distance and the role played by the presence of a nonconstant tip local DOS on STS data. This investigation allows us to ascertain strengths and weaknesses of the existing methods and leads to an optimized and improved strategy which we propose for the analysis of STS data. We tested our conclusions on STS measurements of the Si(111)-7×7 and Au(111) surfaces, acquired with W and Cr tips.

DOI: 10.1103/PhysRevB.79.045404 PACS number(s): 73.20.At, 73.40.Gk, 68.37.Ef

I. INTRODUCTION

The possibility of measuring the local (down to atomic resolution) electron density of states (DOS) of a surface performing the so-called scanning tunneling spectroscopy (STS) is among the most attractive features of the scanning tunneling microscope.[1–6] The fundamental physical quantities acquired are the tunneling current $I(V)$ and the differential conductivity $dI(V)/dV$, both as a function of the applied bias V. In order to obtain quantitative information about the investigated sample, an appropriate treatment of STS data is required. Early attempts in this direction have been proposed soon after the invention of STS, mainly making simple use of available experimental data. By far, among the others, the mostly adopted estimate of the sample local density of states (LDOS) has become the quantity $(dI/dV)/(I/V)$, namely, the differential conductivity divided by the total conductivity.[7] On the other hand, a theoretical description of the tunneling current is definitely required to understand the specific relation among the sample LDOS and the STS quantities, with the goal of identifying the best recovery procedure. In the literature STS experiments are commonly interpreted with descriptions mostly based on a one-dimensional (1D) Wentzel-Kramers-Brillouin (WKB) expression of the tunneling current,[8,9] leading to a number of proposed procedures for the extraction of the sample LDOS,[10–13] thanks to which significant advances in understanding of STS data have been made. Nevertheless these investigations still present important limitations and a number of important open issues have to be faced.

This paper is devoted to these subjects. After a presentation, in Sec. II, of the actual relevant state of the art, we investigate a number of important open questions, with the goal of obtaining a general procedure to interpret STS data; these issues will be discussed in Sec. III. Then, in order to demonstrate the potentialities of the developed ideas, they will be applied to different real experimental situations (Sec. IV). Concluding remarks are given in Sec. V.

II. THEORETICAL FRAMEWORK

The various methods which have been proposed so far for the recovery of the sample LDOS from STS measurements are founded and can be discussed on the basis of the following expression of the tunneling current:[8,9]

$$I(V) = A\int_0^{eV} T(\varepsilon, V, z)\rho_s(\varepsilon)\rho_t(\varepsilon - eV)d\varepsilon. \tag{1}$$

Here ρ_s and ρ_t are the sample and tip LDOSs, respectively, V is the bias, applied to the sample with respect to the tip, A is a proportionality dimensional coefficient which includes the numerical constants and the tip-sample interaction area, and T is a barrier transmission coefficient which, using a 1D-WKB trapezoidal approximation, can be written as

$$T(\varepsilon, V, z) = \exp\left[-2z\sqrt{\frac{2m}{\hbar^2}\left(\Phi + \frac{eV}{2} - \varepsilon\right)}\right], \tag{2}$$

where z is the tip-sample distance and Φ is the effective work function. This equation can be justified within the framework of the transfer Hamiltonian approach.[8,9,14,15]

From Eq. (1) we get an expression for the differential conductivity dI/dV which is, together with $I(V)$, the other quantity measured in STS experiments,

$$\frac{dI}{d(eV)} = A\left[T(eV,V,z)\rho_s(eV)\rho_t(0) + \int_0^{eV} \rho_s(\varepsilon)\frac{d[T(\varepsilon,V,z)\rho_t(\varepsilon - eV)]}{d(eV)}d\varepsilon \right]. \quad (3)$$

We see that two different terms contribute to the differential conductivity. The quantity of interest, namely, the sample LDOS at the energy selected by the applied bias, $\rho_s(eV)$, is contained in the first term of the right-hand side of Eq. (3). The second one is a *background* term that arises from the voltage dependence of the transmission coefficient as well as from a nonconstant tip LDOS. The general problem of an STS experiment is to properly extract the sample LDOS contained in a nontrivial way in the differential conductivity, as evident in Eq. (3).

A number of methods have been proposed to face this crucial issue.[7,10–13] Historically, the first one is due to Stroscio *et al.*[7] who argued about the possibility of removing the effects of the voltage dependence of the tunneling coefficient, normalizing the differential conductivity to the total conductivity I/V.[16,17] Interpreting this procedure with the present 1D-WKB description leads to the expression

$$\frac{dI/dV}{I/V} = \frac{\rho_s(eV)\rho_t(0) + \int_0^{eV} \frac{\rho_s(\varepsilon)}{T(eV,V,z)}\frac{d}{d(eV)}[T(\varepsilon,V,z)\rho_t(\varepsilon - eV)]d\varepsilon}{\frac{1}{eV}\int_0^{eV} \frac{T(\varepsilon,V,z)}{T(eV,V,z)}\rho_s(\varepsilon)\rho_t(\varepsilon - eV)d\varepsilon}. \quad (4)$$

From Eq. (4) it is clear that such normalized differential conductivity is not simply related to the sample LDOS. However, in many experimental situations, especially in the case of semiconducting surfaces, this method leads to results that are qualitatively in agreement with surface LDOS simulated or measured with other spectroscopy techniques. For this reason, even if this treatment lacks strong theoretical foundation, it has become a very common tool for presentation and interpretation of STS data.

A first refinement has been provided in the work of Ukraintsev.[10] Starting from Eq. (3) he showed the possibility of writing a symmetric expression of dI/dV with respect to tip and sample LDOSs. From the resulting expression, an approximate form of the differential conductivity can be obtained, neglecting the effects coming from the background term,

$$\frac{dI}{d(eV)} \simeq A[T(eV,V,z)\rho_s(eV)\rho_t(0) + T(0,V,z)\rho_s(0)\rho_t(-eV)]. \quad (5)$$

From this expression an estimate of sample and tip LDOSs can be performed, dividing dI/dV by the transmission coefficient $T_{\mathrm{sym}}=A[T(eV,V,z)+T(0,V,z)]$ and exploiting the peculiar dependence of T_{sym} on V. The resulting estimates for the sample and tip LDOSs are

$$\rho_s(eV) \propto \frac{dI/dV}{T_{\mathrm{sym}}} \quad (V>0) \quad \rho_t(-eV) \propto \frac{dI/dV}{T_{\mathrm{sym}}} \quad (V<0). \quad (6)$$

This method then provides an approximate treatment for the analysis of *unoccupied* states for both the sample and the tip. From Eqs. (2) and (5) it follows that T_{sym} is symmetrical in the applied voltage while dI/dV curve should not since this feature is also governed by the LDOS of the tip and the sample at the Fermi level, as it can be observed in Eq. (5). So, another possibility is to normalize the differential conductivity using an asymmetric expression for the transmission coefficient $T_{\mathrm{as}}=A_1T(eV,V,z)+A_2T(0,V,z)$. Both T_{sym} and T_{as} are strongly influenced by the tip-sample distance z, so it is necessary to make an appropriate choice for this parameter. This problem will be discussed in detail in Sec. III.

Koslowski *et al.*[12] further elaborated Eq. (3) in order to provide a more quantitative treatment of the background term and produce an expression more explicitly related to the sample LDOS. Using the 1D-WKB expression of T and the mean value theorem for integrals, it follows that

$$A\int_0^{eV} \rho_s(\varepsilon)\rho_t(\varepsilon - eV)\frac{d[T(\varepsilon,V,z)]}{dV}d\varepsilon = -f(z,V)I, \quad (7)$$

where the function $f(z,V)=ez\sqrt{m/2\hbar^2[\Phi+eV/2-\bar{\varepsilon}(V)]}$ [$\bar{\varepsilon}(V)$ depending on the particular system considered] will be further discussed in Sec. III A. With this expression it is possible to relate the background term in Eq. (3) with available data of the tunneling current if it is assumed that the tip LDOS is constant. In these conditions, the extraction of the sample LDOS then follows from Eqs. (1)–(3) and (7), leading to the following relation:

$$\rho_s(eV) = \frac{1}{AT(eV,V,z)\rho_t(0)}\left[\frac{dI}{d(eV)} + \frac{1}{e}f(z,V)I(V)\right]. \quad (8)$$

Finally, the possibility of numerically resuming the sample LDOS has been recently discussed.[12,13] In Ref. 12 from Eq. (3) the problem is formulated in terms of Volterra equations and is numerically investigated. A method for the extraction of both the sample and tip LDOSs is proposed and discussed, together with some intrinsic difficulties which

have to be faced following this approach. In Ref. 13 a numerical method is developed starting directly from Eq. (1) and is applied to the case of STS measurements of organic layers, still assuming that the tip LDOS is constant. In that work, the problem of properly estimating the tip-sample distance from experimental STS data is considered, referring to the particular case of organic samples.

From this discussion it follows that several important issues, which still require investigation in order to establish a solid connection of the STS theory with real STS experiments, emerge naturally: (i) the need of a general and possibly simple evaluation procedure for the effective tip-sample distance z and barrier work function Φ that is of primary importance in every normalization method based on the 1D-WKB description; (ii) the investigation of the effects coming from a possible nonconstant tip LDOS on STS data analysis; (iii) a proper comparison of the various normalization procedures in order to ascertain strengths and weaknesses of the existing methods and to identify an optimized and improved strategy which can be used for the STS analysis; and (iv) the application of this analysis to real experimental STS data. In Secs. III–V of the paper, all these aspects will be discussed and developed.

III. DISCUSSION

A. Improvements of the physical model and estimate of WKB parameters

As discussed in Sec. II, in order to perform analysis of STS dI/dV data with methods different from the normalization to the total conductivity, it is necessary to have a procedure for estimating effective WKB parameters. First, we need an estimation for the A coefficient. This parameter contains the effective tip-sample interaction area and the numerical dimensional constant. It acts as a bridge between the tip and the sample LDOS in Eq. (1) and the measured tunneling current. Because this parameter is only a proportional coefficient, we choose its value in order to make dI/dV, T_{sym}, $f(z,V)I(V)$, and $AT(eV,V,z)$ on the same order of magnitude. The estimation for the distance z between tip and sample and the equivalent work function Φ requires further considerations. Both parameters affect the bias dependence of the transmission coefficient in the 1D WKB description [Eq. (2)], and consequently they influence the features of the normalized spectra. It is important to realize the intrinsic difficulties and limitations which arise if attempts are made to extract these quantities directly from experiments.

In the frame of the WKB approach, the independent variation in these parameters produces similar effects on the transmission coefficient; so, it is possible to assume for the sake of simplicity an arbitrary reasonable value for one parameter (e.g., work function), focusing our analysis on the variation in the other one only[13] (alternatively, the work function can be measured with specific techniques or it can be separately estimated[18]). The aim of this section is to provide a simple but consistent strategy to face this problem, discussing also how the estimated tip-sample distance z affects the recovered spectra. The simplifying assumption of a constant tip LDOS will be initially considered, deferring to Sec. III B for the discussion of the more general case. We identified two different procedures that can be used for estimating z, which will be called in the following *fitting* procedure and *matching* procedure, respectively.

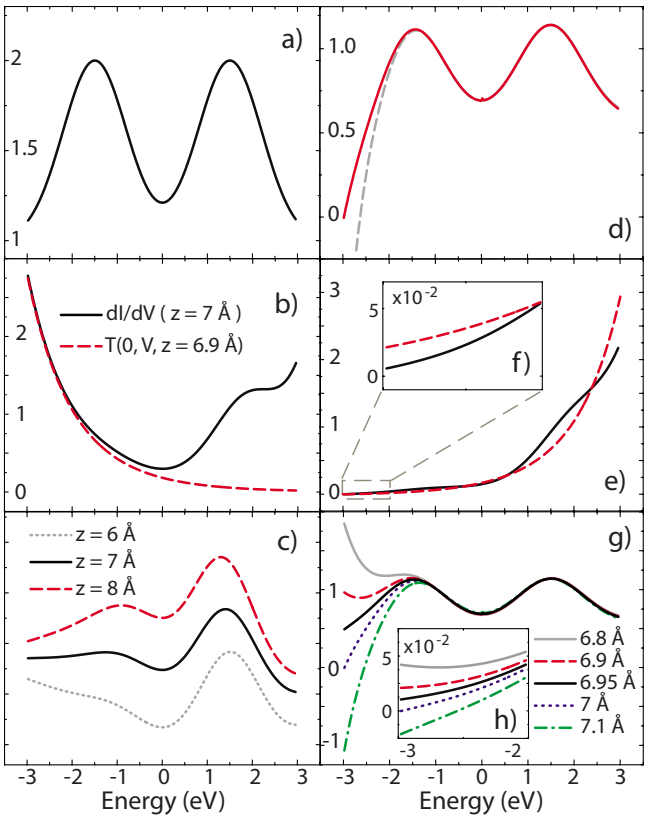

FIG. 1. (Color online) Estimate of WKB parameters. (a) Model sample LDOS. (b) Simulated dI/dV (black solid line) using $z=7$ Å and $\Phi=4.5$ eV and corresponding fit with $AT(0,V,z)$ (red dashed line); estimate gives $z=6.85$ Å. (c) Normalized dI/dV using Eq. (6) with $z=6$ Å (gray dotted line), $z=7$ Å (black solid line), and $z=8$ Å (red dashed line). (d) Normalized dI/dV using Eq. (8) with different $f(z,V)$ from Eq. (9) (dashed gray line) and Eq. (10) (solid red line). (e) $dI/dV+f(z,V)I(V)$ (black solid line) and $AT(eV,V,z)$ (red dashed line) using $z=6.95$ Å and $\Phi=4.5$ eV. Inset (f): magnification of the negative tails. (g) Normalized dI/dV using Eq. (8) with different z values. Inset (h): magnification of the tails of the $dI/dV+f(z,V)I(V)$ construction.

Fitting procedure. A first possibility, originally proposed in Ref. 10 by Ukraintsev, is to extract z performing a fit of the tails of dI/dV data with the symmetric or asymmetric combination of transmission coefficients T (as discussed in Sec. II). Best results are obtained by fitting the curves in the bias region far from the Fermi level, where the characteristic exponential behavior becomes clearly dominant. Very few attempts in this direction have been tried using experimental data.[19,20] Generally speaking, problems in performing this method arise when small bias intervals are considered and, above all, when structures of sample and/or tip LDOS present in the dI/dV curve are predominant and mask the exponential behavior in the entire bias interval. As an example of this effect, in Fig. 1(b) we show the dI/dV curve simulated using Eq. (1) from a model sample LDOS [Fig. 1(a)] composed by two Gaussian peaks with a constant back-

ground (and constant tip LDOS). This simulation is performed using $z=7$ Å and $\Phi=4.5$ eV. The positive voltage region of the curve is strongly modulated by the nonconstant sample unoccupied states and no satisfying fitting of tails is possible, neither with symmetrical nor asymmetrical T. This kind of problem can be overcome performing a fit only of the negative part of the dI/dV curve, which is less affected by structures of the sample LDOS. Applying the fitting procedure to the considered example, a value for z of 6.85 Å is obtained, in good agreement with the correct parameter. Using this information, it then becomes possible to normalize the spectra using the symmetrical combination T_{sym}. However, distortions of the tail, often caused by the presence of surface-projected bulk states, could generate uncertainty in the recovery of the effective tip-sample distance. In order to evaluate the effects of a noncorrect estimation on normalized curves, we plot in Fig. 1(c) different reconstructed spectra obtained with different trial tip-sample distances z and using Eq. (6). A shift in the peaks of about 100–200 meV is present when the estimated distance differs from the real one and a distortion in the shape of the negative bias part of the curve is also visible. However, it can be concluded that this normalization procedure does not generate critical problems if the estimated distance is varied in a range of ± 1 Å with respect to the correct value, and it is therefore capable of providing a useful qualitative insight of STS data in the considered kind of situations.

Matching procedure. We propose an alternative approach, which can be realized starting from Eq. (8) and exploiting quite general arguments. We first present an improvement of the analysis performed in Ref. 12. The analytical expression of the $f(z,V)$ [see Eq. (7)] obtained in this work assuming constant tip and sample LDOSs and applying the generalized mean value theorem is

$$f(z,V) = e\frac{z_n}{4\sqrt{\Phi}}\left(1+\frac{(2\sqrt{\Phi}z_n+3)(eV)^2}{96\Phi^2}\right), \tag{9}$$

where $z_n \equiv 2(2m/\hbar^2)^{1/2}z$. This expression is calculated evaluating integral (7) in the second-order approximation. We obtain an improved estimate of the background term by performing a full analytical integration of the same equations under the same assumptions, leading to the expression

$$f(z,V) = e\frac{z_n^2}{4}\frac{\exp(a)-\exp(b)}{(1-a)\exp(a)-(1-b)\exp(b)}, \tag{10}$$

with $a=-z_n(\Phi-eV/2)^{1/2}$ and $b=-z_n(\Phi+eV/2)^{1/2}$. Both these expressions can be used in the attempt of recovering the sample LDOS via Eq. (8). In Fig. 1(d) we show the difference in recovered spectra using second-order-evaluated coefficient and our analytical improvement starting from the dI/dV simulated curve of Fig. 1(b) (in both normalizations we use the correct simulated value of z and Φ). Equation (10) for $f(z,V)$ provides a better reconstruction of the LDOS in the negative region.

Now, we again consider the problem of the estimation of the WKB parameters. From Eq. (8), it can be easily verified that $dI/dV+f(z,V)I(V)$, which depends on z, must be well defined in sign, namely, it must be a positive quantity over the entire bias interval. This requirement provides an upper limit for z. Possible values of z contained in a very small range below this upper limit produce a strong variation in the negative tail of $dI/dV+f(z,V)I(V)$. It is then appropriate to make the physical requirement that the quantity $[dI/dV+f(z,V)I(V)]/AT$ remain on the same order of magnitude over the entire considered energy interval, thus avoiding the reconstructed tail of the LDOS to become unphysically large with respect to the rest of the spectrum. This requirement can be satisfied if z is such that $[dI/dV+f(z,V)I(V)]/AT \lesssim 1$. In conclusion, we propose to evaluate a proper interval of z requiring $0 \leq [dI/dV+f(z,V)I(V)]/AT \lesssim 1$. This procedure generally leads to a very small interval. As an example, we analyze the same simulated case described in the fitting procedure according to the proposed method. In Fig. 1(e), we show the curve $dI/dV+f(z,V)I(V)$ using an effective tip-sample distance of 6.95 Å. It is visible that, using this value, the curve remains positive in the whole interval. The most critical part of this construction is in the negative voltage region in which the transmission coefficient becomes about 3 orders of magnitude smaller than in the positive voltage region. In the inset of Fig. 1(f), both $dI/dV+f(z,V)I(V)$ and $AT(eV,V,z)$ between -2 and -3 V are magnified and it is visible that, using this value for z, both curves remain on the same order of magnitude. This produces the best recovery for sample LDOS [see solid black line curve in Fig. 1(g)].

To get a deeper insight in the effect of an error Δz on the estimate, we can evaluate analytically the variation in Eq. (8) when $\tilde{z} \equiv z+\Delta z$ is used instead of z,

$$\frac{1}{AT(eV,V,\tilde{z})}\left[\frac{dI}{dV}+f(\tilde{z},V)I(V)\right] = \frac{\rho_s(eV)\rho_t(0)}{T(\Delta z,V)}+\frac{\Delta f}{AT(z,V)T(\Delta z,V)}I(V), \tag{11}$$

where $\Delta f=f(\tilde{z})-f(z)$. For $\Delta z<z$, the most important contribution comes from the last term and its behavior is mainly visible at negative bias, where $1/T(z,V)$ becomes larger. Since Δf is a monotonic function of Δz while $I(V)$ is negative for negative bias, the overall effect is the addition of a positive (negative) term in the negative bias region when a lower (larger) value of the tip-sample distance is estimated.

These remarks are presented in Fig. 1(g), where the distance z is varied for the same STS curve (while Φ is kept constant at 4.5 eV). In the inset of Fig. 1(h) the voltage region between -2 and -3 V for all the $dI/dV+f(z,V)I(V)$ corresponding to different z is magnified; here the differences induced by small variation in the estimated distance as well as the critical value above which the curve becomes negative are visible. Effect of this variation in z parameter in normalized dI/dV is visible in Fig. 1(g). Satisfying the condition previously discussed, it is possible to identify an interval for the estimation of z between 6.9 and 7 Å, in satisfactory agreement with the real value used to simulate the dI/dV curve. In this sense, the proposed method can also be used to normalize using Eq. (6), as further discussed in Secs. III B and III C. Also, it is interesting to note that using these extracted z values, the shape of normalized curves in the region above -1.5 V does not change [Fig. 1(g)]. The recon-

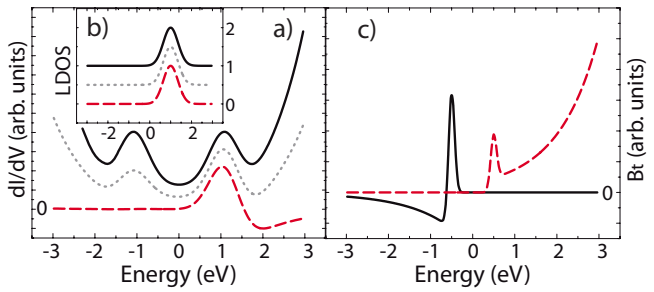

FIG. 2. (Color online) Effects of nonconstant tip LDOS. (a) Simulated dI/dV using different sample LDOS shown in the inset [(b) model tip LDOS is composed of a constant background and a Gaussian peak at +1 eV]. Panel (c) B_t from Eq. (16) in the case of a sharp peak in the tip unoccupied (solid black line) and occupied states (dashed red line), respectively.

structed curve closely follows the sample LDOS.

To summarize the results of the present discussion, if a constant tip LDOS can be assumed, it is possible to use the negative tail of the quantity $dI/dV+f(z,V)I(V)$ in order to obtain a robust estimate of the tip-sample distance, imposing the conditions $0 \leq [dI/dV+f(z,V)I(V)]/AT \lesssim 1$. This estimate usually grants a good reconstruction of the sample LDOS using Eq. (8).

B. Effects of the tip electronic structure

We have so far assumed a constant tip LDOS. Real tips are likely to possess a nontrivial energetic structure, as revealed by experimental[21] and numerical investigations[22–25] of tips LDOS and by STS real data.[26] In these conditions, new contributions to the differential conductivity arise [see Eq. (3)], the effect of which on the extraction of the sample LDOS should be investigated. Generally speaking, the tip electronic structure appears clearly in STS spectra when the sample LDOS at the Fermi level is not negligible, as in the case of a metal surface, because the tip LDOS term is essentially weighted by $\rho_s(0)$, as it can be observed from the approximated expression contained in Eq. (5). In order to show this important behavior, in Fig. 2(a) we display three different simulated dI/dV curves all referring to systems in which both the sample and the tip LDOS consist of a single Gaussian peak in the unoccupied energy region over a constant background [Fig. 2(b)]. Increasing the sample background term [and consequently $\rho_s(0)$] without varying the tip LDOS (peak at +1 eV in the unoccupied states over a constant background) leads to a corresponding growth of the peak in the negative bias region of the differential conductivity, which is generated by the tip electronic structure. Moreover, other effects caused by the presence of both nontrivial tip and sample LDOSs can appear in STS spectra, as it will be discussed in the following.

In the 1D-WKB approach, nonconstant tip LDOS effects are contained in the last term of Eq. (3). It is possible to rewrite this expression, using Eq. (7), in order to generalize the results of Sec. III A valid in the constant tip LDOS case, obtaining for the differential conductivity,

$$\frac{dI}{d(eV)} = AT(eV,V,z)\rho_s(eV)\rho_t(0) - \frac{1}{e}f(z,V)I(V) + B_t, \tag{12}$$

where the last contribution

$$B_t = A\int_0^{eV} \rho_s(\varepsilon)T(\varepsilon,V,z)\frac{d[\rho_t(\varepsilon - eV)]}{d(eV)}d\varepsilon \tag{13}$$

describes the tip LDOS-related effects.

In order to get a first insight, it can be useful to analyze this term introducing some simplifying assumptions. Let us first consider the case in which the sample LDOS $\rho_s(\varepsilon)$ can be considered almost constant in the energetic interval in which $d[\rho_t(\varepsilon - eV)]/d(eV) \neq 0$. Integrating by parts [Eq. (13)], B_t is given by

$$\begin{aligned} B_t &\propto A\Bigg[T(0,V,z)\rho_t(-eV) - T(eV,V,z)\rho_t(0) \\ &\quad + \int_0^{eV}\frac{d[T(\varepsilon,V,z)]}{d\varepsilon}\rho_t(\varepsilon - eV)d\varepsilon\Bigg] \\ &\approx AT(0,V,z)\rho_t(-eV) - AT(eV,V,z)\rho_t(0) + \frac{2}{e}f(z,V)I, \end{aligned} \tag{14}$$

where the last approximate and simplified expression follows using arguments similar to those leading to Eq. (7). Accordingly, Eq. (8) can be generalized, and we obtain

$$\begin{aligned} &\frac{1}{AT(eV,V,z)\rho_t(0)}\left[\frac{dI}{d(eV)} + \frac{1}{e}f(z,V)I(V)\right] \\ &\quad \approx \rho_s(eV) + \frac{\rho_s(0)}{\rho_t(0)}\frac{T(0,V,z)}{T(eV,V,z)}\rho_t(-eV). \end{aligned} \tag{15}$$

Equation (15) is not simply proportional to $\rho_s(eV)$ and it exhibits a strong dependence on the sign of the applied bias; in particular, this normalization could strongly enhance the $\rho_t(-eV)$ term at negative bias, where the ratio $T(0,V)/T(eV,V)$ becomes greater as the bias decreases. Since ρ_t is evaluated at $-eV$, this normalization procedure strongly enhances the visibility of the tip unoccupied states. These properties could be used in order to recognize the presence of a nonconstant tip electronic LDOS in a given experimental situation.

In order to analyze in more detail the present situation, we further assume that the tip is characterized by well-defined peaks which, for the sake of simplicity, can be approximated by Dirac functions. In other words, we assume that $\rho_t \cong \bar{\rho}_t + \eta\Sigma_\mu\delta(\varepsilon - \varepsilon_\mu)$, where η is an appropriate constant used to match units. For a given μ, B_t does not give any contribution in the interval between Fermi level and ε_μ, while for $|eV| > |\varepsilon_\mu|$ Eq. (13) reduces to

$$B_t \propto T(0,V,z)\Delta\rho_t(-eV) - \eta\sum_{\mu}\frac{|\varepsilon_\mu|}{\varepsilon_\mu}\left|\frac{d[T(\varepsilon,V,z)]}{d\varepsilon}\right|_{\varepsilon=eV+\varepsilon_\mu}, \tag{16}$$

where $\Delta\rho_t \equiv \rho_t - \bar{\rho}_t$. The effect of a delta state in tip LDOS depends on its position with respect to the Fermi level, as represented in Fig. 2(c), where the quantity in Eq. (16) is shown for two different choices of ε_μ. In particular, a peak in the unoccupied states generates a negative contribution in the negative bias range which increases (in absolute value) with z. This could strongly interfere with z estimation by the matching procedure, leading to values which are significantly lower than the real one, as discussed below in more detail.

If it cannot be assumed that the sample LDOS is almost constant in the region where $d[\rho_t(\varepsilon-eV)]/d(eV) \neq 0$, it is possible to investigate the properties of B_t still assuming that $\rho_t \cong \bar{\rho}_t + \eta\Sigma_\mu\delta(\varepsilon-\varepsilon_\mu)$, leading to

$$B_t \propto T(0,V,z)\Delta\rho_t(-eV)\rho_s(0) + \eta\sum_{\mu}\left[\rho_s(\varepsilon)\frac{d}{d(\varepsilon)}T(\varepsilon,V,z) + T(\varepsilon,V,z)\frac{d}{d(\varepsilon)}\rho_s(\varepsilon)\right]_{\varepsilon=\varepsilon_\mu+eV} \tag{17}$$

and a corresponding variation in Eq. (15). From these relations several conclusions can be drawn. At positive bias, when $T(\varepsilon,V)$ increases exponentially with V, we expect the presence of new contributions to the differential conductivity,[27] related to the sample LDOS and its energy derivative at the energy $(\varepsilon_\mu+eV)$. This last term is dominant because the ratio $T/T' = (\Phi - eV/2 - \varepsilon_\mu)^{1/2}/z(2m/\hbar^2)^{1/2}$ is larger than one in usual experimental conditions. At negative bias, tip and sample LDOSs exchange their role and it follows that a nonconstant sample LDOS can induce extra features related to the tip which can be observed in this region. We want to stress that the presence of satellite peaks does not depend on $\rho_s(0)$. As a consequence these additional contributes should be visible also for sample surfaces with an energetic gap.

We performed a series of numerical simulations in order to ascertain the effects induced by the presence of a nonconstant tip LDOS suggested by the above analysis. We organize our discussion starting with two different and particularly interesting situations in which both tip and sample LDOSs are nonconstant:

(a) nonconstant features in the tip occupied and sample unoccupied states (therefore this is the case in which both systems produce nonconstant contributions in the positive voltage region of dI/dV);

b) both structures are nonconstant in their unoccupied states.

These two cases are investigated using, for both the tip and the sample, a model LDOS composed by a constant background plus a Gaussian peak and simulating the resulting STS dI/dV and normalized spectra.

(a) First, we analyze the presence of a peak in the occupied states of the tip. In particular, we consider a sample LDOS with a sharp Gaussian peak at $\varepsilon_s = +1.5$ eV and a tip

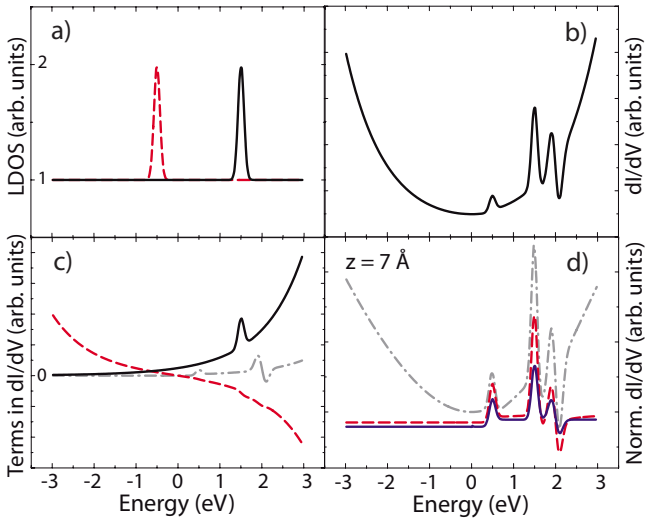

FIG. 3. (Color online) Effects of a nonconstant tip occupied LDOS. (a) Sample (solid black line) and tip LDOSs (red dashed line). (b) Simulated dI/dV ($z=7$ Å and $\Phi=4.5$ eV). (c) The three contributions to dI/dV [see Eq. (12)], the first one containing $\rho_s(eV)$ (solid black line), the second one proportional to $-I(V)$ (dashed red line), and the third containing nonconstant tip effect (dashed-dotted gray line). (d) Comparison of the normalized dI/dV using normalization to I/V (dashed-dotted gray line), using Eq. (6) (dashed red line) and Eq. (8) (solid blue line).

LDOS with a peak at $\varepsilon_\mu = -0.5$ eV [Fig. 3(a)]. The corresponding dI/dV, shown in Fig. 3(b), reveals the presence of both the sample peak at +1.5 eV and the tip peak at +0.5 eV. In addition, an extra feature can be observed at $\varepsilon_s + |\varepsilon_\mu| = +2$ eV that is mainly due to the derivative of the sample LDOS shifted by 0.5 eV, according to the general discussion of Eqs. (15) and (17). In Fig. 3(c) the three contributions to the dI/dV curve defined in Eq. (12) are shown. The first contribution comes from the ρ_s term times the transmission coefficient $T(eV,V)$, the second is the term proportional to the tunneling current, while the third contains the effects of the nonconstant LDOS tip, namely, the tip LDOS as well as the extra feature resulting from the convolution of the LDOS of the sample and the tip. It is important to note that since in the considered situation all the various additional contributions appear only in the positive bias region, the procedures proposed in Sec. III A for the estimation of the effective tip-sample distance still remain valid and can be used. The resulting normalized spectra are shown in Fig. 3(d).

(b) We now consider the case of a peak in the unoccupied states of the tip LDOS. To understand the main features of this configuration, we simulate a condition where both tip and sample LDOSs exhibit a peak at +1 eV superimposed on different constant backgrounds [see Fig. 4(a)]. The corresponding dI/dV [Fig. 4(b)] shows that the typical exponential behavior is strongly modulated and an optimal exponential fit for z recovery using either the negative or positive bias region data cannot be performed. Looking at Fig. 4(c), the three contributions to dI/dV, as described by Eq. (12), can be distinguished. In particular, a negative contribution is visible in the last part of the negative bias region. This term is the

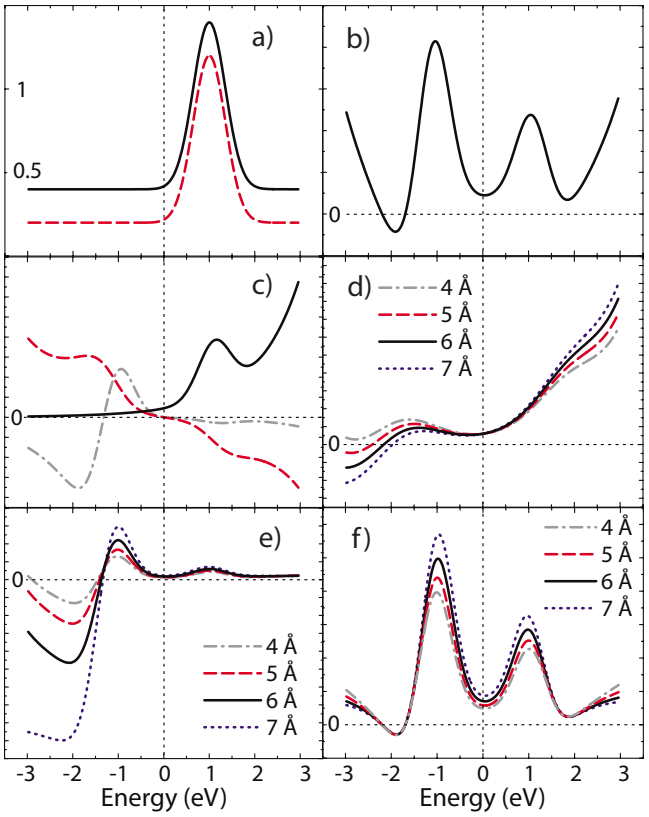

FIG. 4. (Color online) Effect of nonconstant tip unoccupied LDOS. (a) Sample (solid black line) and tip LDOS (red dashed line). (b) Simulated dI/dV (z=7 Å and Φ=4.5 eV). (c) The three contributions to dI/dV [see Eq. (12)], the first one containing $\rho_s(eV)$ (solid black line), the second one proportional to $-I(V)$ (dashed red line), and the third containing nonconstant tip effect (dashed-dotted gray line). (d) $dI/dV+f(z,V)I(V)$ constructions obtained using different effective z. [(e) and (f)] Corresponding normalized dI/dV curves using Eqs. (8) and (6), respectively.

one described in Eq. (16). In this situation, the constrain $dI/dV+f(z,V)I(V)>0$ discussed in Sec. III A in general does not apply and is not verified for the correct value of the tip-sample distance. This problem arises from the fact that Eqs. (9) and (10) have been obtained under the assumption of constant tip and sample LDOSs. Even though these expressions work well also when the sample LDOS is not constant, they are not adequate to model the presence of a nonconstant LDOS in the tip unoccupied states. In principle, a correct estimate should be possible by re-evaluating the function $f(z,V)$ in the case of a model tip LDOS (e.g., the form previously discussed). However, this solution requires specific assumption on the tip electronic structure. Another possibility of overcoming this problem is to evaluate the same $f(z,V)$ given by Eq. (10) at an effective $\tilde{z}=z+\Delta z$. As already noted in Sec. III A, an underestimation of z produces a positive contribution in the negative bias region and it would balance the negative contribution coming from the last term of Eq. (13). Now, $\tilde{z}$ is no longer a physical value but it works as an effective parameter. (For example, in the situation described in Fig. 4(a), the constrain $dI/dV+f(z,V)I(V)>0$ is satisfied for $\tilde{z}<4$ Å while z=7 Å.) This effective parameter is obtained performing a fit of the entire curve (not only the region with a clear exponential behavior) with an asymmetric combination of T coefficient and using the resulting estimate as an effective parameter for normalization. The presence of a negative contribution to the differential conductivity also influences the normalized results. A large negative value region, visible in Fig. 4(e), is present in normalized dI/dV using Eq. (8) if the correct z parameter is used, while it disappears using smaller estimated distances. Moreover, the tip electronic structures are magnified in the negative region, as expected from Eq. (15). On the contrary, normalization using Eq. (6) produces spectra that are less affected by the estimated value and the relative amplitude of the tip and the sample LDOS are not significantly altered [Fig. 4(f)]. These differences in the normalized data produced by different methods can be used as a hint to qualitatively distinguish if a feature observed in dI/dV data comes from tip or sample LDOS.

We also want to point out that the negative term in Eq. (16) should be responsible for a negative differential conductivity (NDR) in the negative bias region. This effect, which is the dual of what has been previously observed by Wagner *et al.*[13] for positive sample-tip bias, should be observed if a pronounced structure in the unoccupied tip states is combined with a large value of $\rho_s(0)$. In this case, the B_t term can overcome in absolute value the other two terms in Eq. (12), producing negative values in the dI/dV curves. As an example of this effect, the dI/dV curve relative to the last discussed case [see Fig. 4(b)] shows a NDR region at about −2 eV.

We conclude the present discussion by commenting on the remaining possible situations not considered yet. A system where tip and sample LDOSs are nonconstant in the occupied and unoccupied states, respectively (therefore, they produce effects in the negative voltage interval of the dI/dV curve), can be simply considered the dual of case (a) previously analyzed. In particular, here extra features can arise and consist in a term proportional to the tip LDOS and its derivative at energies selected by the energetic positions of the sample peaks. Moreover, problems arise in evaluation of the tip-sample distance because of the influence of both nonconstant tip LDOSs and extra features in the negative bias region, but it is possible to perform a fitting of the positive tail of the differential conductivity, extracting a satisfactory estimate of z. Finally, we note that no particular observations are needed in the case in which both structures are nonconstant only in their respective occupied states, this situation being qualitatively similar to the constant tip LDOS case.

C. Comparison of the normalization methods

Our analysis allows the identification of various strategies to treat STS data. In order to reach a coherent picture and propose a comprehensive approach, we now want to compare the various possibilities paying attention mainly to two aspects: (i) capability in estimating a correct effective value for the required tip-sample distance and (ii) reliability and accuracy in recovering the sample and tip LDOS.

First, we summarize what has been previously observed about the recovery of the tip-sample distance:

Constant tip LDOS. This is the best situation: an estimate of z can be obtained with great accuracy both fitting the negative bias tail of the dI/dV curve (if the considered bias interval is sufficiently large) and/or satisfying the condition $0 \leq [dI/dV + f(z,V)I(V)]/AT \lesssim 1$. In this case, z can be estimated with an accuracy of 0.1–0.2 Å.

Nonconstant tip LDOS. Four possible qualitatively distinct combinations of sample and tip LDOSs have been described in which the main differences are dictated by the relative position of tip and sample peaks in the unoccupied and/or occupied states. If the tip has no pronounced structures in the unoccupied states, the same considerations made for the constant tip LDOS case still apply. On the contrary, if the tip shows electronic features in the unoccupied region (producing effects in the negative bias interval of the differential conductivity), the negative tail of the dI/dV curve does not allow an appropriate estimate of z. Then, it is possible either to fit the positive tail of the curve (if the sample presents no evident structures in this region) or, elsewhere, to perform a fit of the entire curve to extract a trial effective value of the tip-sample distance which, in this case, acts as an effective parameter.

The effect of a noncorrect estimated z and the presence of a nonconstant tip LDOS can be considered for a critical comparison of the various normalization methods. We summarize in four main points what has been discussed.

(a) In the presence of a constant tip LDOS (and a correct estimated distance), use of Eq. (8) leads to a correct reconstruction of the spectrum while Eq. (6) produces a shift of about 0.1–0.2 eV and a pronounced damping of the sample peak amplitude in the occupied states.

(b) The negative bias region is a critical issue for the use of Eq. (8), and small variations in the estimate of the effective tip-sample distance produce a strong effect on the resulting recovered LDOS. For this reason, in this region the reconstruction obtained using Eq. (6) provides a more reliable method.

(c) In the presence of one or more pronounced peaks in the unoccupied states of the tip, Eq. (8) produces a strong amplification of the tip features as well as unphysically large (or negative) values of the reconstructed LDOS in the negative bias region. On the other hand, Eq. (6) treats symmetrically the tip and sample unoccupied states, as pointed out in Sec. II. Conversely, a strong irregularity and peak amplification obtained using Eq. (8) for an unknown spectrum should be an indication of the presence of a nonconstant tip LDOS. In this case, Eq. (8) produces meaningful spectra only in the positive bias region, while it is possible to analyze the region $V<0$ using Eq. (6).

(d) A noncorrect z estimate, caused by structured tip LDOS in the unoccupied region, produces a systematic shift of the peaks toward greater energy values with both procedures.

IV. APPLICATION TO EXPERIMENTAL DATA

From the preceding discussion we developed a general strategy for the analysis of STS data, which is worth testing on real measurements. In this section we consider this issue, applying these methods to real STS spectra of well-known surfaces. Compared with previous investigations of experimental data, here the main purpose is to discuss the role played by the presence of tip-related structures in STS data. In order to measure some of the predicted tip-related effects, it is particularly convenient to analyze systems with the following requirements: (a) a nonvanishing LDOS at Fermi level, as discussed at the beginning of Sec. III B, and (b) a well-known electronic structure, in order to distinguish the possible tip extra features in STS spectra. Among the others, Si(111)-7×7 and Au(111) surfaces fully satisfy these conditions. In order to reveal the possible different behavior of a given scanning tunneling microscopy (STM) tip in an STS experiment, we probed these surfaces using both standard bulk W tips and also recently proposed bulk Cr tips.[28] All the experimental data have been acquired at room temperature (RT) using an Omicron Variable Temperature -STM in UHV conditions ($<5.0\times10^{-11}$ mbar). All the presented spectra are the result of an average over tens of equivalent curves.

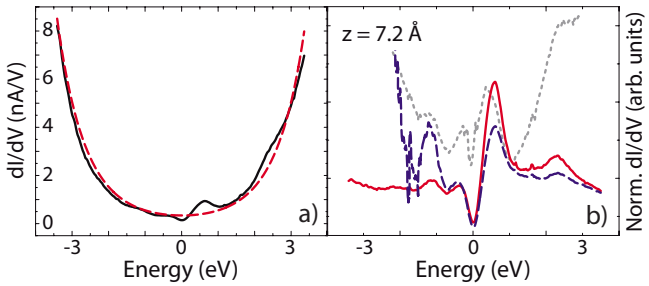

FIG. 5. (Color online) STS measures of Si(111)-7×7 surface. (a) dI/dV (solid black line) and asymmetric T_{as} fit (dashed red line) (z=7.2 Å and Φ=4.5 eV). STS spectrum has been obtained, averaging over all the nonequivalent atomic position. (b) Comparison of the normalized dI/dV using normalization to I/V (dashed-dotted gray line), Eq. (6) (solid red line), and Eq. (8) (dashed blue line). Parameters have been estimated using the *fitting* procedure.

We start discussing a typical STS spectrum of the Si(111)-7×7 surface. From photoemission spectroscopy[29–33] and STS measurements,[34–36] it is known that this surface presents a complex structure and seven nonequivalent atomic positions. Three clear peaks can be found in the surface DOS; at +0.5 and at −0.3 eV surface states relative to the adatom sites are found, while at about −1 eV a state attributed to rest atom states is present. Another large surface feature is situated near 2 eV, and it is superposed to surface-projected bulk bands. Using a bulk Cr tip we have been able to acquire spatially averaged dI/dV curves in a wide range of applied bias from −3.5 to 3.5 V at V_b=1 V and I_t=0.5 nA [Fig. 5(a)]. Exponential tails are clearly visible in the differential conductivity. In this case, no peaks appear other than those expected from the sample LDOS; we can then assume that the tip electronic structure used in this experiment is almost constant in energy in the considered interval. We extracted the tip-sample distance z using both the fitting [see Fig. 5(a)] and the matching procedure. In both cases we found a value of 7.2 Å. After having determined the needed parameters, in Fig. 5(b) we compare the curves obtained, normalizing the dI/dV to the total conductivity and using the other methods discussed in this paper. The normalization to

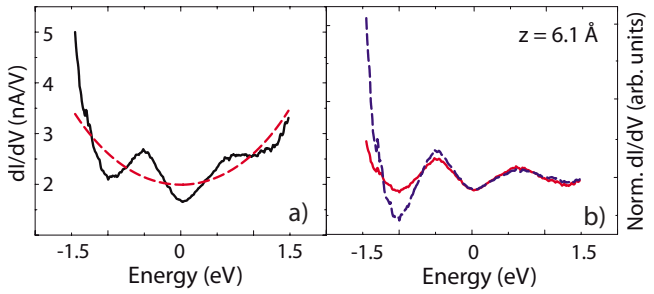

FIG. 6. (Color online) STS measures of Au(111) surface. (a) dI/dV spectrum of the Au(111) reconstructed surface (solid black line) and asymmetrical T_{as} fit (z=6.1 Å and Φ=4.5 eV). (b) Comparison of the normalized dI/dV using Eq. (6) (solid red line) and Eq. (8) (dashed blue line). Parameters have been estimated using the fitting procedure.

the total conductivity is always affected by a shift in the recovered energetic position of the sample peaks. Moreover, as already observed, sample occupied states are always dampened using Eq. (6), while they seem to be better recovered using Eq. (8). It is interesting to note how this recovery can be achieved even for an occupied state of the sample well below the Fermi level, as the one lying at −1 eV. At even lower values, however, only the use of Eq. (6) produces reliable values, while curves normalized with the other procedure become quite irregular, in agreement with the considerations developed in Sec. III C (and also because the limited dynamic range in data acquisition significantly contributes to the irregular behavior in this negative bias region).

In order to show an example of STS data in which the presence of the tip LDOS is clearly visible, we discuss a measurement on the Au(111) surface. This system has a Shockley state that contributes to the LDOS from −0.5 eV up to the Fermi level, while no other features are expected in the interval between −1 and 1 eV; outside this range, surface-projected states begin to dominate the LDOS spectrum[37,38] (for a proper recovery of an ideal Shockley state using a specific normalization procedure that takes into account the peculiar energetic behavior of such surface states see Ref. 12). In Fig. 6(a) we show a dI/dV curve acquired in the bias interval from −1.5 to 1.5 V at V_b=−0.45 V and I_t=0.9 nA using a W tip. We observe the contribution of the Shockley peak and another structure at +0.6 eV. Since we do not expect any pronounced feature in the positive bias interval from the sample LDOS, we attribute this second structure to the tip LDOS. Comparing this spectrum to what has been shown in Fig. 2, we can interpret this magnification of the tip electronic features, observing that the presence of the Shockley states strongly enhances the sample LDOS at Fermi level. In this case the electronic structures of both the tip and the sample are in their respective occupied states. Due to the limited bias range we performed the z estimation, fitting the whole curve with the asymmetrical combination of the T coefficient [Fig. 6(a)]. The corresponding normalized curves are shown in Fig. 6(b).

We conclude the discussion of experimental cases presenting an investigation of spatially resolved STS spectra obtained on a set of equivalent atomic positions [corner-faulted (CoF) adatoms] of the Si(111)-7×7 surface acquired with a W tip. Generally speaking, even if STS is capable of probing electronic states potentially with atomic resolution, it is quite usual, especially in RT measurements, to collect electrons coming from atoms in a slightly larger region of space. It is therefore common, when probing adatom electronic states on the Si(111)-7×7 surface, to get information also from the surface-projected bands and also from the rest atoms. A typical normalized spectrum of the CoF atomic sites is presented in Fig. 7(a), where the two adatom states previously described are clearly visible. Minor contribution comes from the rest atom state (−1 eV) and surface-projected band (above +0.5 eV). This kind of measurement is in full agreement with other works presented in the literature.[35,36,39] In one particular experimental condition we obtained the STS dI/dV curve shown in Fig. 7(b), which shows an extra peak at +1.2 eV and a dampened zone in the negative bias region. It is interesting to note that similar results have been reported in the literature.[26,40] Since these

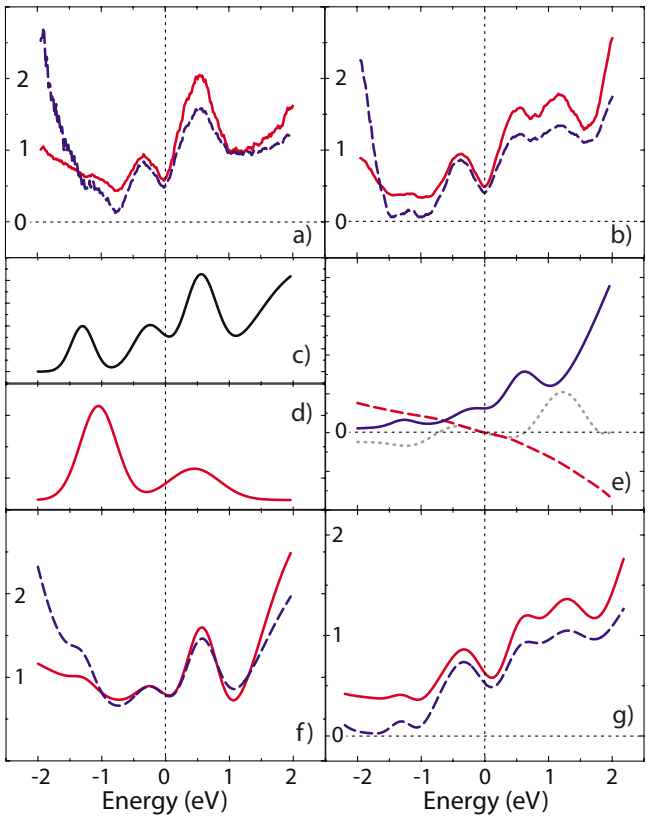

FIG. 7. (Color online) STS measures of Si(111)-7×7 corner-faulted adatoms. [(a) and (b) V_b=1 V, I_t=0.5 nA.] Different normalized STS spectra using Eq. (6) (solid red line) and Eq. (8) (dashed blue line). The estimated effective tip sample distances are in the two cases z=6 Å and z=5 Å. (c) Model Si corner-faulted adatom LDOS. (d) Model W tip LDOS. (e) The three contributions to simulated dI/dV [see Eq. (12)] (z=5 Å and Φ=4.5 eV), the first one containing $\rho_s(eV)$ (solid black line), the second one proportional to $-I(V)$ (dashed red line), and the third containing nonconstant tip effects (dashed-dotted gray line). [(f) and (g)] Normalized simulated dI/dV curves using, respectively, a constant tip LDOS and the tip LDOS of panel (d). STS curves are normalized using Eq. (6) (solid red line) and Eq. (8) (dashed blue line).

structures are not expected and they are not always measured in other spectra on equivalent sites, we attribute these features to nonconstant tip LDOS effects due to a particular tip configuration. We simulated an ideal situation of sample and tip LDOSs that could reproduce the experimental data on the basis of the known features of the Si(111)-7×7 system and the general discussion performed in Sec. III B. In particular, we considered a sample LDOS composed by three Gaussian peaks, a band edge, and a small constant background [see Fig. 7(c)]. We first assume a flat tip LDOS: in these conditions, the conventional STS spectra on CoF adatoms can be reproduced using Eq. (1) with satisfactory agreement, as can be observed comparing Figs. 7(a) and 7(e). Then, in order to interpret the unconventional spectrum shown in Fig. 7(b), we model a different tip LDOS with a constant background and a sum of two Gaussian peaks: one at $\varepsilon_{tu}=0.5$ eV and one at $\varepsilon_{to}=-1$ eV, as shown in Fig. 7(d). The amplitude and position of the peaks have been chosen in order to reproduce the experimental STS observations. According to Eqs. (15)–(17) and Figs. 3 and 4, we expect to find several additional contributions in the recovered spectrum coming from the quantity B_t: (i) a peak at the position $eV=-\varepsilon_{tu}$; (ii) a reduced value of extracted LDOS in the region below $eV=-\varepsilon_{tu}$; (iii) a peak at the position $eV=-\varepsilon_{to}$; and (iv) a contribution proportional to the sample LDOS and its derivative shifted by an amount equal to ε_{to}. In the considered bias interval, this last contribution should produce an additional feature at the energetic position $\varepsilon_{s1}+|\varepsilon_{to}|=1.5$ eV, where $\varepsilon_{s1}=0.5$ eV is the energetic position of the sample adatom unoccupied state. Actually, modeling sample LDOS and the tip LDOS as shown in Figs. 7(c) and 7(d), the quantity B_t [Fig. 7(e)] contains all these features, in particular, the dominant term coming from the derivative of the sample LDOS at ε_{s1} produces a distinct feature around +1.2 eV. These considerations can consequently explain the observed STS spectrum. Figures 7(b) and 7(g) show the experimental and modeled normalized curves, respectively, and a satisfactory agreement can be readily appreciated. It is interesting to note that an existing numerical investigation reported in Ref. 41 shows that a W tip can actually arrange its last apex atoms in order to have a relatively smooth LDOS with two sharp peaks at −0.9 and 0.2 eV.

V. CONCLUSIONS

In this paper the crucial problem of the interpretation of the physical information contained in an STS measurement has been considered within the framework of a 1D-WKB description of the tunneling current. Facing a number of important issues, such as the correct estimation of the required physical parameters and the effects of a nonconstant tip LDOS on STS spectra, we have been able to perform a critical analysis and an extension of the methods so far considered in the literature. In this way, we are led to propose an optimized and improved general strategy for the analysis of STS data, which has also been used to interpret experimental STS data from different surfaces [Si(111)-7×7 and Au(111)] and with different STM tips (W and Cr). From the study of such experimental data, the importance of considering the consequences of a nonconstant tip LDOS is particularly evident. An interesting improvement in the recovery of tip and sample LDOSs would be achieved, combining the results obtained in this work with approaches based on the use of numerical methods, such as those proposed in Refs. 12 and 13.

As a further development of the present investigation, these results can be generalized in order to properly include the three-dimensional (3D) spatial properties of the full system (sample and tip), following a similar path but starting from a more general expression of the tunneling current and derivative, such as those which can be obtained within the framework of the transfer Hamiltonian approach.[15]

[1] *Scanning Tunneling Microscopy*, edited by J. A. Stroscio and W. J. Kaiser (Academic, Boston, 1993).
[2] C. J. Chen, *Introduction to Scanning Tunneling Microscopy*, 2nd ed. (Oxford University Press, New York, 2008).
[3] C. Bai, *Scanning Tunneling Microscopy and Its Applications*, 2nd ed. (Springer, Berlin, 2000).
[4] *Scanning Probe Microscopy and Spectroscopy*, edited by D. Bonnell (Wiley, New York, 2001).
[5] G. A. D. Briggs and A. J. Fisher, Surf. Sci. Rep. **33**, 1 (1999).
[6] J. M. Blanco, F. Flores, and R. Pèrez, Prog. Surf. Sci. **81**, 403 (2006).
[7] J. A. Stroscio, R. M. Feenstra, and A. P. Fein, Phys. Rev. Lett. **58**, 1668 (1987).
[8] C. B. Duke, *Tunneling in Solids* (Academic, New York, 1969).
[9] J. A. Appelbaum and W. F. Brinkman, Phys. Rev. **186**, 464 (1969).
[10] V. A. Ukraintsev, Phys. Rev. B **53**, 11176 (1996).
[11] N. Li, M. Zinke-Allmang, and H. Iwasaki, Surf. Sci. **554**, 253 (2004).
[12] B. Koslowski, C. Dietrich, A. Tschetschetkin, and P. Ziemann, Phys. Rev. B **75**, 035421 (2007).
[13] C. Wagner, R. Franke, and T. Fritz, Phys. Rev. B **75**, 235432 (2007).
[14] J. Bardeen, Phys. Rev. Lett. **6**, 57 (1961).
[15] M. Passoni and C. E. Bottani, Phys. Rev. B **76**, 115404 (2007).
[16] A. Selloni, P. Carnevali, E. Tosatti, and C. D. Chen, Phys. Rev. B **31**, 2602 (1985).
[17] N. D. Lang, Phys. Rev. B **34**, 5947 (1986).
[18] J. J. W. M. Rosink, M. A. Blauw, L. J. Geerligs, E. van der Drift, and S. Radelaar, Phys. Rev. B **62**, 10459 (2000).
[19] M. M. J. Bischoff, T. Yamada, A. J. Quinn, and H. van Kempen, Surf. Sci. **501**, 155 (2002).
[20] T. K. Yamada, M. M. J. Bischoff, G. M. M. Heijnen, T. Mizoguchi, and H. van Kempen, Phys. Rev. Lett. **90**, 056803 (2003).
[21] N. Garcia, V. T. Binh, and S. T. Purcell, Surf. Sci. **293**, L884 (1993).
[22] M. Tsukada, K. Kobayashi, and N. Isshiki, Surf. Sci. **242**, 12 (1991).

[23] W. A. Hofer and J. Redinger, Surf. Sci. **447**, 51 (2000); W. A. Hofer, J. Redinger, A. Biedermann, and P. Varga, *ibid.* **466**, L795 (2000); W. A. Hofer and A. Garcia-Lekue, Phys. Rev. B **71**, 085401 (2005).
[24] W. A. Hofer, A. S. Foster, and A. L. Shluger, Rev. Mod. Phys. **75**, 1287 (2003).
[25] W. A. Hofer, J. Redinger, and P. Varga, Solid State Commun. **113**, 245 (1999); W. A. Hofer, J. Redinger, and R. Podloucky, Phys. Rev. B **64**, 125108 (2001).
[26] J. P. Pelz, Phys. Rev. B **43**, 6746 (1991).
[27] G. Hörmandinger, Phys. Rev. B **49**, 13897 (1994).
[28] A. Li Bassi, C. S. Casari, D. Cattaneo, F. Donati, S. Foglio, M. Passoni, C. E. Bottani, P. Biagioni, A. Brambilla, M. Finazzi, F. Ciccacci, and L. Duò, Appl. Phys. Lett. **91**, 173120 (2007).
[29] R. I. G. Uhrberg, G. V. Hansson, J. M. Nicholls, P. E. S. Persson, and S. A. Flodström, Phys. Rev. B **31**, 3805 (1985).
[30] J. M. Nicholls and B. Reihl, Phys. Rev. B **36**, 8071 (1987).
[31] R. I. G. Uhrberg, T. Kaurila, and Y.-C. Chao, Phys. Rev. B **58**, R1730 (1998).
[32] R. Losio, K. N. Altmann, and F. J. Himpsel, Phys. Rev. B **61**, 10845 (2000).
[33] R. Negishi, M. Suzuki, and Y. Shigeta, J. Appl. Phys. **98**, 063712 (2005).
[34] R. J. Hamers, R. M. Tromp, and J. E. Demuth, Phys. Rev. Lett. **56**, 1972 (1986); Surf. Sci. **181**, 346 (1987).
[35] R. Wolkow and Ph. Avouris, Phys. Rev. Lett. **60**, 1049 (1988); Ph. Avouris and R. Wolkow, Phys. Rev. B **39**, 5091 (1989).
[36] R. Negishi and Y. Shigeta, Surf. Sci. **507–510**, 582 (2002).
[37] D. P. Woodruff, W. A. Royer, and N. V. Smith, Phys. Rev. B **34**, 764 (1986).
[38] S. D. Kevan and R. H. Gaylord, Phys. Rev. B **36**, 5809 (1987).
[39] J. Mysliveček, A. Stróżecka, J. Steffl, P. Sobotík, I. Ošt'ádal and B. Voigtländer, Phys. Rev. B **73**, 161302(R) (2006).
[40] M. Tomitori, K. Sugata, G. Okuyama, and H. Kimata, Surf. Sci. **355**, 21 (1996).
[41] A. L. Vázquez de Parga, O. S. Hernán, R. Miranda, A. Levy Yeyati, N. Mingo, A. Martín-Rodero, and F. Flores, Phys. Rev. Lett. **80**, 357 (1998).